THE PERFORMANCE OF COMPOSITE WOOD/PARTICLEBOARD BEAMS UNDER TWO-POINT LOADING

Jay A. Johnson,[1] *Geza Ifju*, and *Harry W. Rogers*
Department of Forestry and Forest Products, Virginia Polytechnic Institute and State University, Blacksburg, VA 24061

(Received 13 June 1975)

ABSTRACT

Twelve composite wood/particleboard box and I beams were tested under two-point loading. The observed flexural rigidity, EI, was found to be less than the calculated values based on properties of the individual elements. Load bearing capacity was predicted on the basis of the weakest component, which in this study appeared to be the tensile strength of the particleboard. Measured maximum loads were greater than predicted loads. The load-deflection curves were linear to failure, exhibiting virtually no warning signals prior to failure. Failure in many instances was associated with nails used to fabricate the beams. Performance of the beams was estimated to be the equivalent of an intermediate grade 2 × 10 with a 50% strength reduction.

Keywords: *Pinus sp.* (southern pine), *Quercus sp.*, *Nyssa sp.*, *Liriodendron tulipifera*, flexural rigidity, elastic properties, composite beam formulas, failure surfaces, stress concentrations, nails, modulus of elasticity, stress analysis.

LIST OF SYMBOLS

a	Distance between load application and end of the beam
A	Cross-sectional area of a beam segment.
b	Width of a beam segment
c	Distance from the furthest point in a segment to the neutral axis.
d	Distance from the top of a beam segment to the neutral axis.
D	Distance from geometric centroid of a beam segment to the neutral axis.
E	Elastic modulus of a beam segment.
EI	Flexural rigidity of the composite beam.
EQ	Weighted statical moment above an arbitrary plane in the beam.
f, g	Tensile (or compressive), shear strength of a beam segment.
I	Moment of inertia of a beam segment.
k	Composite beam stiffness.
L	Length of the composite beam.
M, V	Moment, vertical shear distributions.
P	Total applied load.
$P^{(1)}_{max}$, $P^{(2)}_{max}$	Maximum applied load for the beam, assuming the material in a particular beam segment is the weakest link in (1) tension (or compression), (2) shear.
Q	Statical moment of a beam segment.
S, T	Coefficients ('section moduli') for the material segments relating the maximum applied load to the tensile (or compressive), shear strength.
x, y	Coordinates for the composite beam with respect to the neutral axis: x, length and y, depth.
$\bar{y}$	Location of the neutral axis with respect to the bottom of the beam.
Y	Distance of geometric centroid of a beam segment to the bottom of the beam.
δ	Composite beam deflection at midspan.
ψ	Geometric factor for beam loading arrangements.
σ, τ	Normal, shear stress acting in a beam segment.
ξ	Ratio of a to L.

Subscripts

i	Beam segment.
k	Beam segment above the i^{th} beam segment.

INTRODUCTION

The idea of manufacturing large structural elements from small pieces of wood is intriguing. A tremendous volume of wood could be utilized that is now considered waste. A new technology can be imagined in which huge beams are

[1] Present address: Weyerhaeuser Company, Tacoma, WA 84801

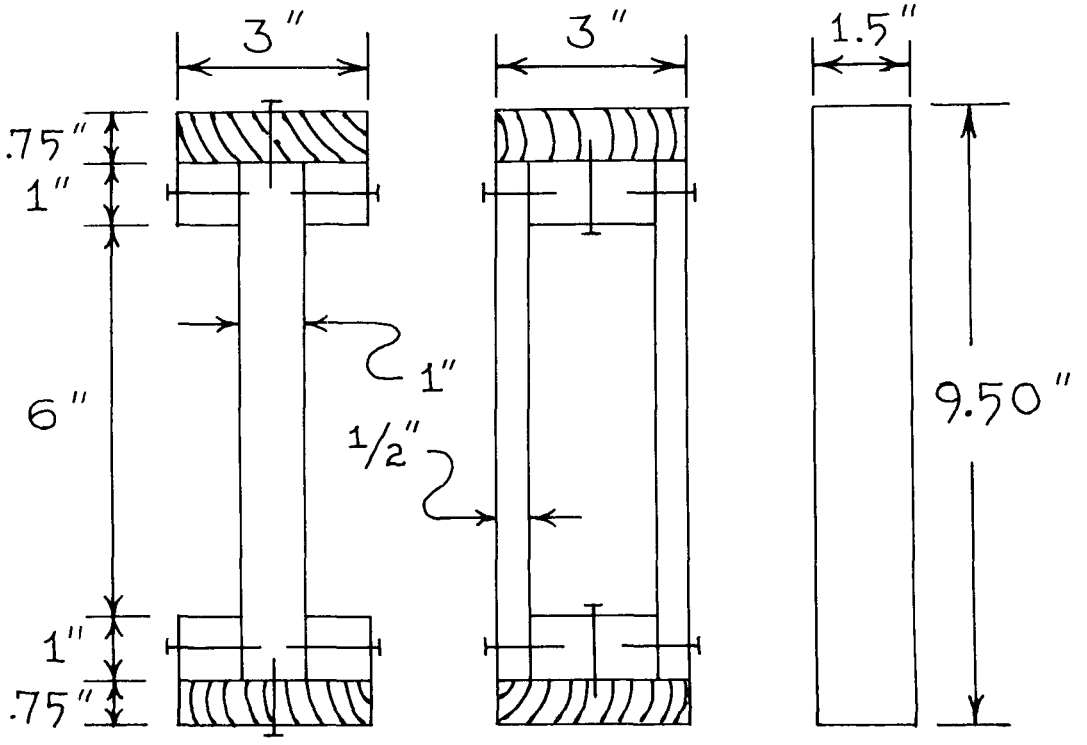

FIG. 1. Cross sections of *two* composite wood/particleboard beams and a 2 × 10.

constructed on-site, incorporating compatible binding materials, and designed for a specific use as dictated by the uniqueness of the resulting structure. Yet, there are many obstacles to be overcome before large structural beams can be made from particles of wood, if in fact, they can be made at all. The inherent weak planes of wood represent one problem and binding systems represent yet another, not to mention, of course, the economics of the situation. These problems notwithstanding, it was felt that an interesting study could be undertaken in which commercially available particleboards could be used as shear webs of box and I beams with clear wood being used as outer flanges taking up much of the tensile and compressive strain energy of the beam. Thus, the purpose of this study was to observe the performance of composite wood/particleboard beams under a two-point loading arrangement and to compare their behavior with the expected behavior of a solid wood structural component, namely, the 2 × 10.

MATERIALS AND METHODS

Two types of beams, box (B) and I (I), were used in this study. Their cross sections are shown in Fig. 1, along with the cross section of a 2 × 10 for comparison. The beams were constructed by gluing strips of southern pine and particleboard together with a room-temperature setting urea formaldehyde resin. Nails, 4d common, were used primarily to hold the strips in place while the glue set. Nail holes were predrilled.

Two types of particleboard were used in the composite beams: a three-layered or structured board (S), Nova-ply, manufactured by the U.S. Plywood Company, and a homogeneous or unstructured board (U), manufactured by the Stuart Lumber Company. The structured board had a nominal

density of 40 lbs/ft^3 and an internal bond strength of approximately 100 psi. The faces, constituting about 20% of the board, were composed of pine flakes with a resin content of approximately 10%. The core consisted of oak and mixed hardwood species (yellow-poplar, gum, etc.) particles. Resin content of the core was 6%. The binder was urea formaldehyde resin. The unstructured board, known commercially as Stuart Board, had a nominal density of 50 lbs/ft^3 and a typical internal bond strength of 100 psi. It was composed of 30% oak and 70% pine with a resin content of 7%. Urea formaldehyde resin was used as a binder and an emulsion was added for water repellency.

Since in-plane tensile and compressive strength values, as well as the in-plane elastic moduli, were not readily available for both types of boards, a number of tension and compression tests were performed to establish characteristic values for these properties. Three groups of tension specimens were used: 1) unstructured board 1 inch thick (U), 2) structured board 1 inch thick (S), and 3) structured board 0.5 inch thick (SA). The samples were 18 inches long and 1 inch wide with tapered wood tabs, 6 inches long, glued to the faces of both ends of the strips. Plywood blocks, 4 inches long, were glued to the wood tabs providing bearing surfaces for the special grips attached to a floor model Instron testing machine used to apply tensile forces to the strips. Elongation of the strips was recorded, using an extensometer (2-inch gauge length). The knife edges of the extensometer were held against the faces of the 6-inch free span of the particleboard specimens.

Four groups of compression samples were used: 1) structured board 1 inch thick (S), 2) unstructured board 1 inch thick (U), 3) structured board 0.5 inch thick with two strips bonded together (SB), and 4) unstructured board 0.5 inch thick with two strips bonded together (UB). The compression specimens were 4 inches long with a cross section of one square inch.

Bending of the composite beams was accomplished with a Tinius Olsen 150,000 lb semi-automatic beam tester. The loading arrangement for the beams tested in this study, along with the appropriate shear, moment, and deflection diagrams, is shown in Fig. 2. Twelve 8-ft-long composite beams were loaded by means of two maple loading blocks (9-inch diameter) located 3 ft from each end and were supported on rollers 6 inches from each end. Deflection at midspan was recorded using a dial micrometer throughout the test at a rate of deflection of 0.01 inches/minute.

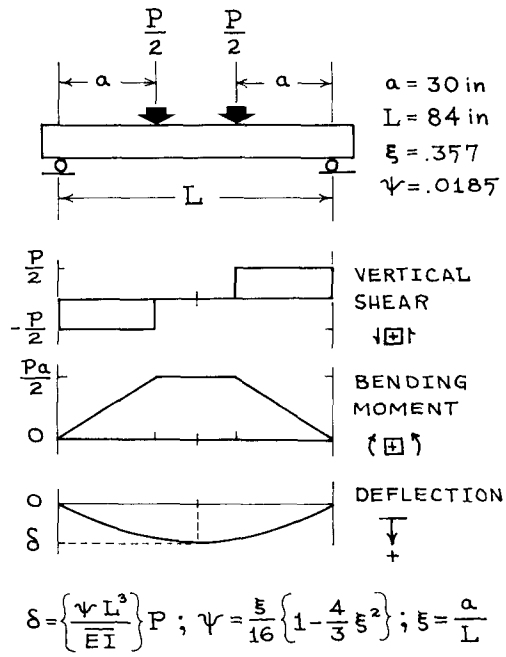

FIG. 2. The loading arrangement used in this study.

THEORY

The expected relationship between the deflection at midspan, δ, and the total load, P, acting on the beam through two load application points is

$$P = k\,\delta \qquad [1]$$

where the stiffness, k, of the composite beams is given by

$$k = \frac{\overline{EI}}{\psi L^3} \qquad [2]$$

with $\overline{EI}$ representing the effective flexural rigidity of the beam; L, the length, and ψ, a geometric factor as given in Fig. 2. This relationship presupposes the beam to consist of ideally elastic materials fused together with perfect bonds. If the elastic properties of the component materials are known, the effective flexural rigidity can be calculated using the parallel axis theorem

$$\overline{EI} = \sum E_i (I_i + A_i D_i^2) \qquad [3]$$

where E_i, I_i, and A_i are the elastic modulus, moment of inertia, and cross-sectional area for each material segment in the cross section of the beam. D_i is the distance between the centroid of each segment and the neutral axis of the overall beam. The location of the neutral axis with respect to the bottom of the beam, $\bar{y}$, is found by balancing the forces acting within the cross section of the beam and is given by

$$\bar{y} = \frac{\sum Y_i E_i A_i}{\sum E_i A_i} \qquad [4]$$

where Y_i is the distance from the centroid of each segment to the bottom of the beam. The box and I beams of Fig. 1 are symmetric with respect to shape and position of the component materials within the cross section, but if the elastic modulus in tension differs from the elastic modulus in compression, the position of the NA will not coincide with the geometric centroid of the cross section. In this study, two of the material segment cross-sectional areas will depend on the location of the neutral axis; consequently, the determination of $\bar{y}$ involves the solution of a quadratic expression. The derivation of the equations used in this study can be found in a report by Johnson et al. (1975).

Normal and shear stresses within the beam are determined with $\bar{y}$ and $\overline{EI}$. Utilizing the standard beam theory assumption that normal strain is proportional to beam curvature and distance from the neutral axis, it can be shown that the maximum normal stress, σ_i, in each material segment of the composite beam is given by

$$\sigma_i = \left(\frac{E_i c_i}{\overline{EI}}\right) M(x) \qquad [5]$$

where c_i is the distance from the furthest point in the material segment to the neutral axis and M(x) is the moment acting at a distance x along the length of the beam. The standard technique for obtaining the resultant shear force acting on any plane parallel to the neutral surface can be used to obtain the shear stress, τ_i, in each material

$$\tau_i = b_i \left(\frac{\overline{EQ}_i}{\overline{EI}}\right) V(x) \qquad [6]$$

where b_i is the width of the material segment, V(x) is the vertical shear acting at the position x, and $\overline{EQ}_i$ is the weighted statical moment above the plane of interest as given by

$$\overline{EQ}_i = E_i Q_i + \sum_{\kappa > i} E_\kappa Q_\kappa \qquad [7]$$

where

$$Q_\kappa = \frac{b_\kappa}{2} (d_\kappa^2 - d_{\kappa-1}^2) \qquad [8]$$

$$Q_i = \frac{b_i}{2} (d_i^2 - y^2) \qquad [9]$$

and d_k is the distance from the neutral axis to the top of the material segment and y is the distance between the neutral plane and the plane of interest.

Since each material segment in the cross section has its own elastic modulus, the normal stress distributions will not be a continuous linear function of beam depth, nor will the shear stress distribution have a

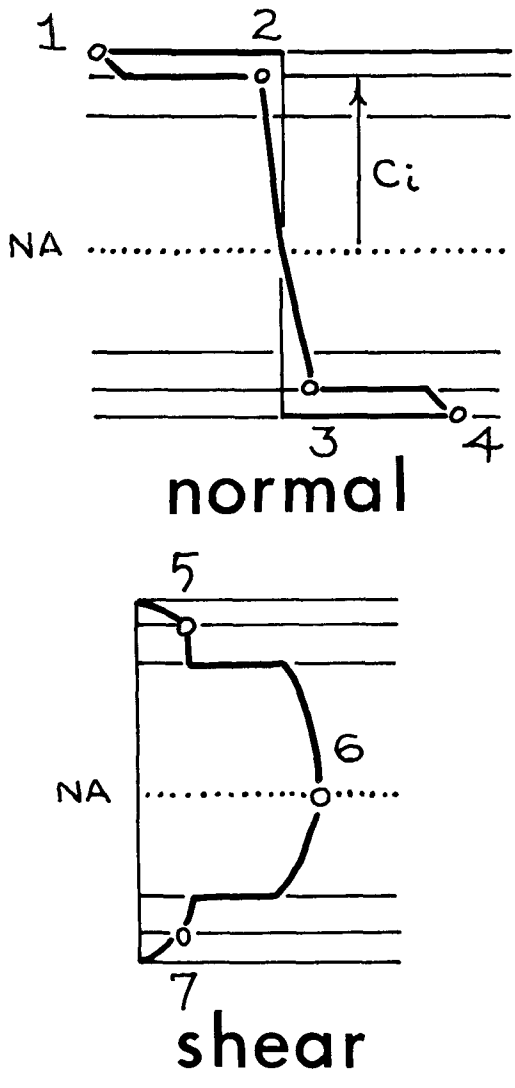

FIG. 3. Stress distributions in a wood/particleboard composite beam.

continuous parabolic shape through the beam height. Calculated stress distributions are shown in Fig. 3 for the box and I beams used in this study using elastic properties of the particleboard and wood differing in compression and tension.

The strength of each material in the cross section of the beam is not expected to be the same; thus if the local stress in a certain segment attains an ultimate value, it will cause failure even though another portion of the beam might be under a larger stress. To predict failure of the beam, therefore, a maximum applied load must be calculated for each material segment, assuming that it is the weakest link in either tension (or compression) or shear. From the resulting set of maximum applied loads calculated for each material segment, the minimum value will represent the load-bearing capacity of the composite beam and will indicate which material segment is the actual weakest link.

A maximum applied load, $P_{max,i}$, based on the tensile (or compressive) strength, f_i, of the i^{th} segment can be found by inserting the maximum moment acting on the beam into Eq. [5] and inverting:

$$P^{(1)}_{MAX,i} = S_i f_i \qquad [10]$$

where

$$S_i = \frac{2}{ac_i}\left(\frac{\overline{EI}}{E_i}\right) \qquad [11]$$

Similarly, another maximum load, $P_{max,i}$, based on the shear strength, g_i, of the i^{th} segment can be found by inserting the maximum vertical shear acting on the beam into Eq. [6] and inverting:

$$P^{(2)}_{MAX,i} = T_i g_i \qquad [12]$$

where

$$T_i = 2b_i\left(\frac{\overline{EI}}{\overline{EQ_i}}\right) \qquad [13]$$

It is convenient to think of S_i and T_i as 'section moduli.' The minimum value of $P^{(j)}_{max,i}$ for j = 1, 2, and all values of i will represent the expected load-bearing capacity of the composite beam.

RESULTS AND DISCUSSION

Particleboard properties

Results of the tension and compression tests are shown in Table 1. The compressive elastic moduli for the structured and

TABLE 1. *Elastic and strength properties of structured and unstructured particleboard tested in tension and compression.*

Sample Group[a]	Elastic Modulus		Ultimate Stress	
	$\bar{x}$ (10^6 psi)	CV (%)	$\bar{x}$ (10^3 psi)	CV (%)
	tension			
U	0.445	20.0	1.08	15.5
S	0.852	16.9	1.10	10.1
SA	0.488	19.8	1.02	19.0
	compression			
U	0.193	7.1	3.22	4.8
UB	0.185	12.4	2.72	15.7
S	0.165	8.5	1.75	5.3
SB	0.188	8.2	1.91	9.2

[a] 10 samples in each group

U: Unstructured, 1" thickness
S: Structured, 1" thickness
SA: Structured, 0.5" thickness
UB: Unstructured, 1" thickness by gluing together two 0.5" boards
SB: Structured, 1" thickness by gluing together two 0.5" boards

unstructured boards are very similar, independent of whether the samples were cut from 1-inch-thick boards or were composed of two 0.5-inch-thick strips glued together. The tensile elastic modulus for both boards is seen to be greater than the compressive elastic modulus. The 1-inch-thick structured board group (S) has a value approximately twice that of the other group. No explanation can be offered for this high value, except that the samples were not randomized, because of the limited amount of available material, and perhaps a particularly stiff board was encountered. If this board was stiffer, however, it did not show any significant strength increase as indicated by the ultimate strength values of the tension specimens. The compressive strengths of both types of boards were greater than the tensile strengths. Also, the unstructured boards were stronger in compression than the structured boards. The stress at the proportional limit was about 60% of the ultimate stress for the tensile samples, 50% for the unstructured compressive samples, and about 70% for the structured, compressive samples. More detailed information concerning the actual force-deflection curves of these materials is found in a report by Johnson et al. (1975).

Comparison of calculated and observed behavior

The results of calculations of $\bar{y}$ and $\overline{EI}$ of the composite beams used in this study, assuming various combinations of elastic moduli for wood and particleboard, are shown in Table 2. The greatest shift in the neutral axis (approximately 0.6 inch) occurs when the compressive modulus is less than the tensile modulus for both wood and particleboard. The difference between the compressive and tensile moduli of particleboard shifts the neutral axis to a greater extent than the difference between the compressive and tensile moduli of wood. Regardless of the neutral axis location, the flexural rigidity is dominated by the elastic

TABLE 2. *Typical calculated values for the distance of the neutral axis (NA) from the bottom of the beam ($\bar{y}$) and the flexural rigidity ($\overline{EI}$) of wood/particleboard composite box and I beams.*

Particleboard	Elastic Modulus[a] $E(10^6$ psi)		Location of NA $\bar{y}$ (in)[c] wood[b]			Flexural Rigidity $\overline{EI}(10^6$ lb-in^2) wood[b]		
	E_t	E_c	I	II	III	I	II	III
unstructured	0.45	0.19	4.42	4.23	4.45	179	188	201
structured	0.49	0.16	4.35	4.14	4.36	179	187	200
average	0.32	0.32	4.75	4.55	4.75	181	191	202

[a] E_t: tensile elastic modulus, E_c: compressive elastic modulus

[b] I: $E_t = 1.75 \times 10^6$ psi and $E_c = 1.75 \times 10^6$ psi

II: $E_t = 2.00 \times 10^6$ psi and $E_c = 1.75 \times 10^6$ psi

III: $E_t = 2.00 \times 10^6$ psi and $E_c = 2.00 \times 10^6$ psi

[c] Geometric center of beam is 4.75" from the extreme fiber

moduli of the wood. In each of the calculations shown in Table 2, the amount of clear wood in the cross section was 27%, but the contribution of the wood, by virtue of its location, to the flexural rigidity of the composite beam in all cases was 85% ± 2%.

(j)

A set of ultimate applied loads $P_{max,i}$ based on the stiffness and strength of the

TABLE 3. *Load-bearing capacity of the wood/particleboard composite beams based on the strength of each component.*

Variable	Type of Particleboard[a]	Position of load calculation (see Figure 3) 1	2	3	4	5	6	7
Distance from NA, c_i (in.)	U	5.27	4.52	3.48	4.23	4.52	0.00	3.48
	S	5.35	4.61	3.39	4.14	4.61	0.00	3.39
		f_i compression[b]		f_i tension[b]		g_i shear[b]		
Strength of i^{th} component f_i or $g_i(10^3$ psi)	U	7.08	3.22	1.08	12.80	1.37	0.75	1.37
	S	7.08	1.75	1.10	12.80	1.37	0.75	1.37
		$P^{(1)}_{max,i}$				$P^{(2)}_{max,i}$		
Maximum load, $P^{(j)}_{max,i}$ $(10^3$ lb)	U	9.6	47.0	8.6	19.0	80.2	12.4	89.1
	S	9.4	29.6	8.3	19.3	78.5	12.4	90.7
Load bearing capacity, $\min\{P^{(j)}_{max,i}\}(10^3$lb)	U	--	--	8.6	--	--	--	--
	S	--	--	8.3	--	--	--	--

[a] U: beams with unstructured particleboard; S: beams with structured particleboard.

[b] Tensile, compressive and shear strength of southern pine were taken from the Wood Handbook (US FPL 1974). An intermediate value of the shear strength for medium density particleboard from the Wood Handbook (US FPL 1974) was used for particleboard.

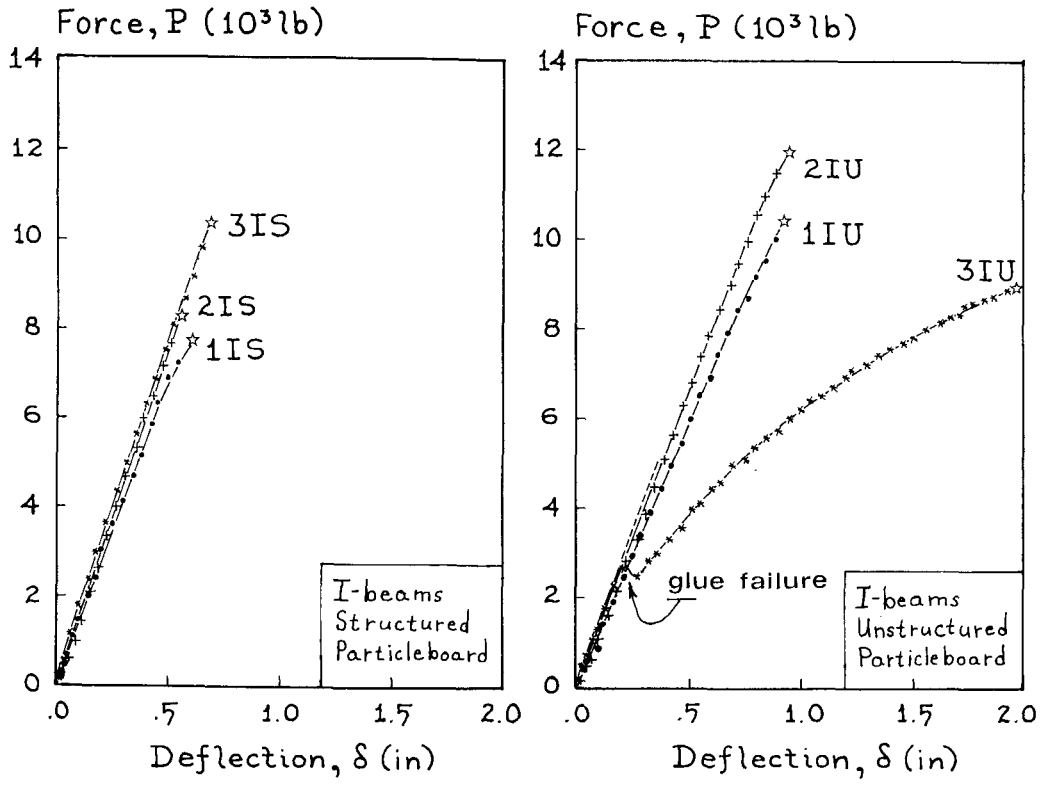

FIG. 4a. Load-deflection curves of wood/particleboard I-beams tested in this study.

wood and particleboard used in this study is shown in Table 3. Flexural rigidities were assumed to be 188 × 10^6 lb-in^2 for the beams with the unstructured particleboard and 187 × 10^6 lb-in^2 for the structured particleboard beams. The tensile, compressive and shear strength values for southern pine were taken from the Wood Handbook (U.S. FPL 1974). A value of 750 psi was assumed for the shear strength across the thickness of the particleboard, which is an intermediate value within the range given in the Wood Handbook (U.S. FPL 1974) for medium density boards (200–1,800 psi). This value also represents a lower bound of edgewise shear strength of ten types of particleboard tested at the U.S. Forest Products Laboratory (McNatt 1973). From these calculations, it can be seen that the expected load-bearing capacity is slightly over 8,000 lb for both types of particleboard beams. The weakest link would be particleboard in tension (position 3 in Fig. 3). It should be noted, however, that if the shear strength of the particleboard is less than 500 psi, the mode of failure would be shear initiated at the neutral axis (position 6) in the span between the load supports and the load application points.

Force-deflection curves of the wood/particleboard composite beams tested in this study are shown in the four diagrams included in Fig. 4. Two of the twelve beams (3IU and 3BU in Fig. 4) failed prematurely but continued to carry a steadily increasing force upon further loading, albeit, at reduced stiffness. The most striking feature about the remaining ten curves is their linearity almost to failure. This, of course, indicates that both materials, wood and particleboard, were efficiently utilized in these types of composite

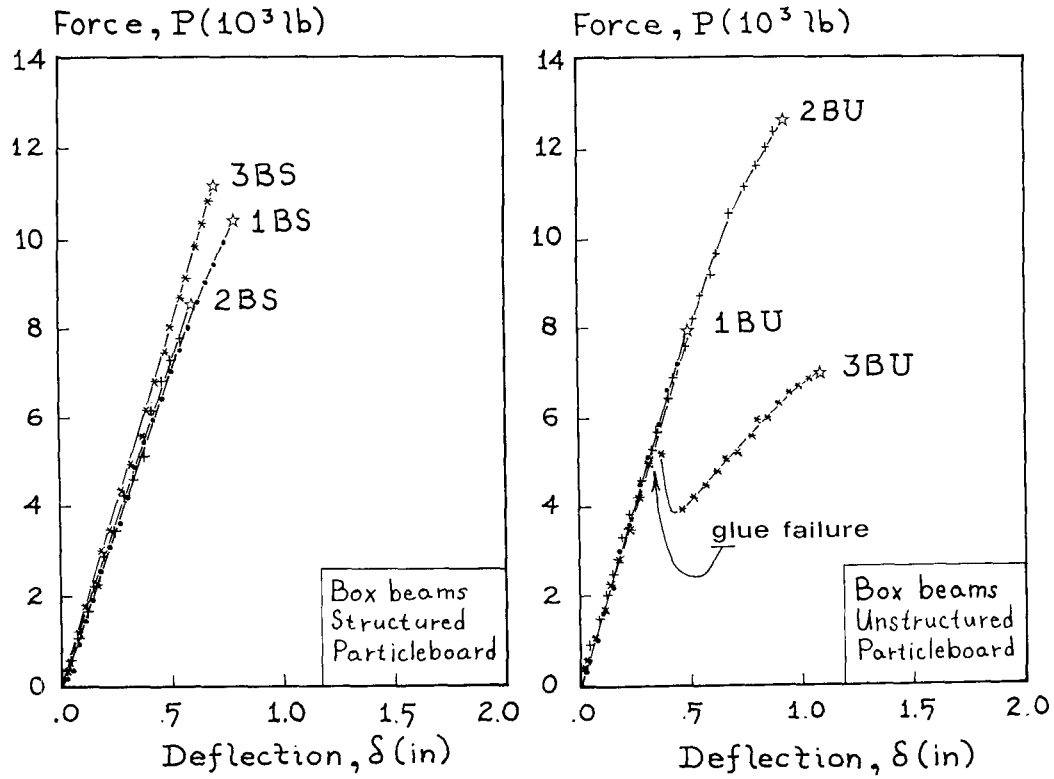

FIG. 4b. Load-deflection curves of six wood/particleboard box beams tested in this study.

TABLE 4. *Observed and expected values of flexural rigidity and load-bearing capacity for wood/particleboard composite beams.*

Beam Type	Flexural Rigidity (10^6 lb-in^2)					Load Bearing Capacity (10^3 lb)				
	Observed				Expected	Observed				Expected
unstructured particleboard	1	2	3	Ave.		1	2	3	Ave.	
I	128	142	143	138		10.4	11.9	2.8[a]	11.2	
Box	176	176	172	174		7.9	12.7	5.2[a]	10.3	
			Average:	156	188			Average:	10.7	8.3
structured particleboard										
I	154	164	172	163		7.7	8.3	10.3	8.8	
Box	155	158	173	162		10.4	8.5	11.1	10.0	
			Average:	162	187			Average:	9.4	8.6

[a]Not included in the average.

beams; their respective stored energies were not dissipated to any great extent prior to failure. As a consequence, however, failure was very abrupt, occurring within a fraction of a second, in an explosive manner, with virtually no advance warnings. Ramaker and Davister (1972) also observed sudden failures, with no apparent previous signs of distress, in three hardboard/wood composite I beams. Their force-deflection curves were also linear to failure.

The observed values of flexural rigidity ($\overline{EI}$) and load-bearing capacity are compared with the expected values in Table 4. The observed $\overline{EI}$ is lower than the calculated values for both particleboard groups, but the observed maximum applied load is higher than expected. The unstructured particleboard beams were slightly stronger, but not quite as stiff as the structured particleboard beams. A southern pine 2 × 10 (1.5″ × 9.5″, an older size) has a flexural rigidity between 190–200 × 10^6 lb-in^2 and if absolutely clear, it might have a load-bearing capacity of approximately 18,000 lbs. Given a lower grade 2 × 10, one in which the strength reduction due to knots, slope-of-grain, etc. amounted to half the clear value, its load capacity would be equivalent to that of the composite beams. Another way of comparing the 2 × 10 with the composite beams is to note that the amount of clear wood in the composite beams is 68% less than in the 2 × 10, but the flexural rigidity is reduced by only 18%. The strength is reduced to 47% of that for a clear 2 × 10 and would be the equivalent of a 2 × 10 of a lower grade.

Failure modes

The failure patterns of the beams were photographed and are shown in Fig. 5. Although difficult to determine, failure of five of the six I beams appeared to initiate in the vicinity of the particleboard and wood segments under tension. On the other hand, only one of the box beams failed in this manner. The flange of one box beam delaminated, two others had shear failures across the particleboard webs near the ends of the beams, and the other box beams had failure initiating in the wood; one in tension, the other in compression. All three I beams made with structured particleboard failed at a load point, and those fabricated from the unstructured boards failed within the midspan. Box beams with structured and those with unstructured particleboard each had one specimen fail within the midspan, one at the load point and one at the support. The diagonal failure surfaces were probably due to a shearing action once the failure was initiated. It was also noted that the crack appeared to run through the individual particleboard segments as though they were a single material showing that the particleboard-to-particleboard glue bond created an essentially unit structure. In some cases, the cracks continued into the wood in approximately the same plane indicating that some of the composite beams were behaving as though they were single material structures.

Many of the fractures occurred in the vicinity of nails. The role of nails as crack initiators is demonstrated in the sequence of photographs of Fig. 6. In all probability, fracture was initiated in the wood at the tip of the nail, Fig. 6a, and spread to the particleboard, running through both webs almost in the same plane, perpendicular to the axis of the beam. The region in the vicinity of the nail tip was explored with an SEM and the overall appearance of the fracture surface is shown in Fig. 6b. The brash texture of the southern pine failure surface indicates a tensile mode of fracture. The region near the tip reveals many broken fibers (Fig. 6c). In particular, the failure surfaces of two fibers are shown in Fig. 6d. Shearing of the cell walls along planes of weakness between the fibril windings is probably responsible for the "tooth" type of appearance of the broken fibers. From other SEM micrographs, it was found that the nails transferred a significant force from the flange to the web as evidenced by the crushed wood particles in the bearing region of the nails. Thus, although the nails were used primarily to hold the flanges in place to allow the glue to set during con-

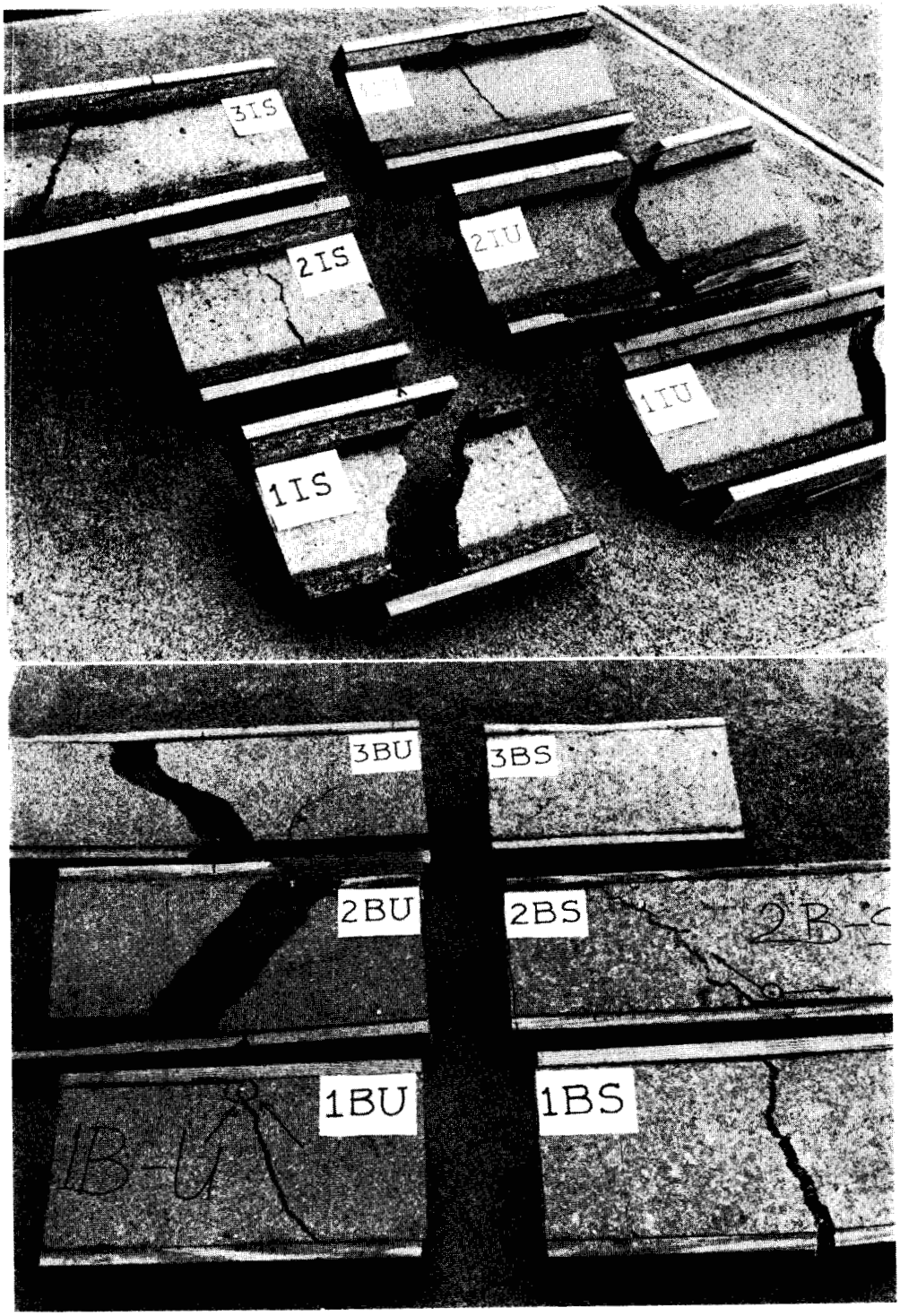

FIG. 5. Failure patterns exhibited by the wood/particleboard composite beams.

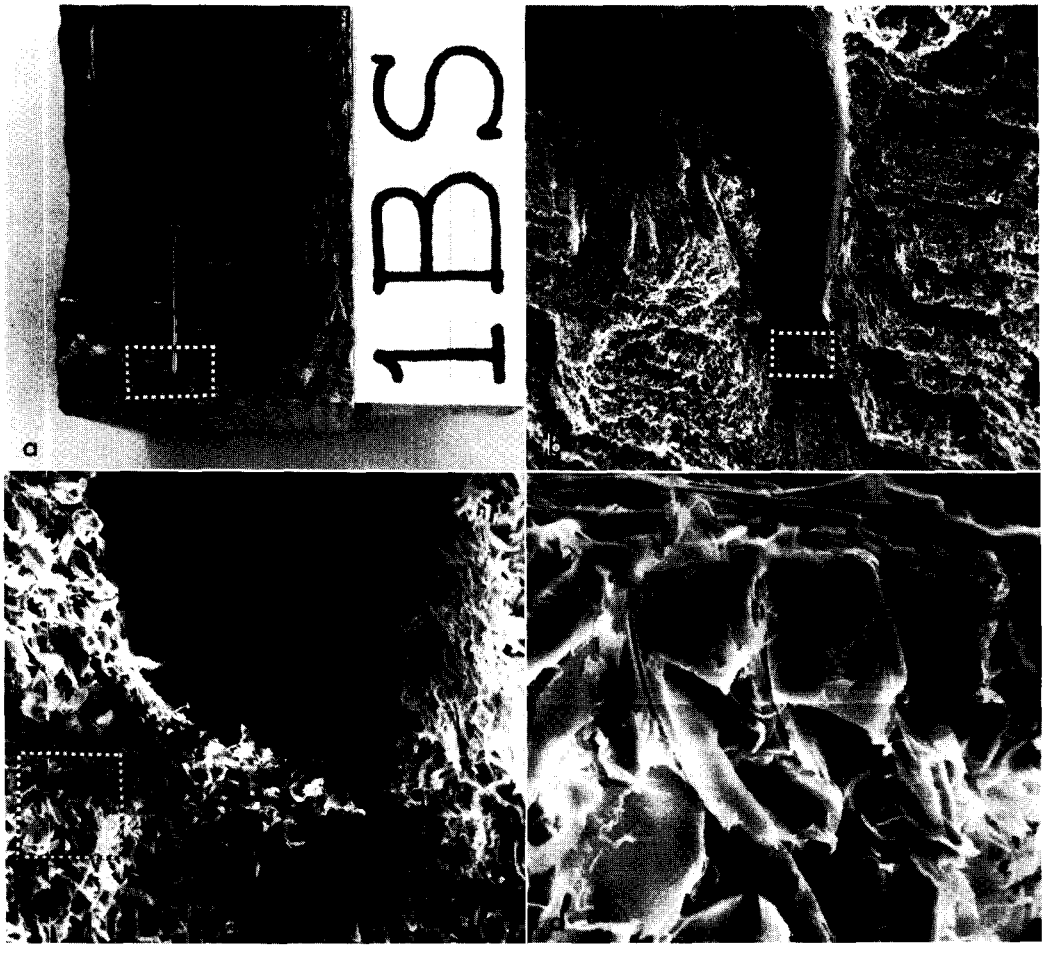

FIG. 6. The fracture surface of a box beam composed of southern pine and a structured particleboard showing the microstructure in the vicinity of a nail. 6a. The tension side of the beam where the tip of the nail may have initiated fracture. 6b. Enlargement of the region, framed in 6a, in the vicinity of the nail tip (nail removed). 6c. Broken fibers near the nail tip, framed in 6b. 6d. Fracture surface of broken fibers, framed in 6c.

struction, they were helpful in terms of preventing interlayer slip between the wood and particleboard. In many instances, however, it was felt that they were also responsible for initiating failure.

CONCLUSIONS

1. The particleboard/wood composite beams used in this study were shown to have roughly 80% of the stiffness and 50% of the strength of a perfectly clear southern pine 2 × 10 (1.5 inches × 9.5 inches) under a two-point loading arrangement, even though the amount of clear wood in the composite beams represented only 30% of amount of wood in the 2 × 10. The observed behavior, however, was probably the equivalent of a lower grade southern pine 2 × 10.

2. The match between theoretical expectations and experimental observations was close but not exact. The flexural rigidity, $\overline{EI}$, was overestimated approximately 10% by theory. The lower measured values for $\overline{EI}$ could be due to interlayer slip be-

tween the wood flange and particleboard web as discussed by Hoyle (1973) and Goodman (1969). The strength of the beams, or the load-bearing capacity, was underestimated by theory.

3. Failure was abrupt with little or no prior warning. Nails, acting as stress concentrators, apparently played a role in crack initiation. The mode of failure was difficult to determine but appeared to start in the tensile region near the wood/particleboard interface. In some cases, the failure surfaces indicated that the composite beams acted as though composed of a single material rather than a collection of individual parts.

4. The force-deflection curves were almost linear to failure; therefore, very little stored energy was lost in the beams due to nonlinear stress-strain behavior. This indicated that the in-plane shear modulus of particleboard was sufficient for use as a shear web of a composite beam verifying Hunt's (1975) conjecture.

REFERENCES

GOODMAN, J. R. 1969. Layered wood systems with interlayer slip. Wood Sci. 1 (3):148–158.

HOYLE, JR., R. J. 1973. Behavior of wood I beams bonded with elastomeric adhesives. Washington State University, Engineering Research Bulletin No. 328. Pullman, Washington.

HUNT, M. O. 1975. Structural particleboard for webs of composite beams? For. Prod. J. 25 (2):55–57.

JOHNSON, J. A., G. IFJU, AND H. W. ROGERS. 1975. The performance of composite wood/particleboard beams under two-point loading. Virginia Polytechnic Institute and State University Wood Science and Technology Report No. VPI-WST 75-1, pp. 17.

MCNATT, J. D. 1973. Basic engineering properties of particleboard. USDA For. Ser. Res. Paper FPL 206. 14 pp. Madison, WI.

RAMAKER, T. J. AND M. D. DAVISTER. 1972. Predicting performance of hardboard in I beams. USDA For. Ser. Res. Paper FPL 185. 13 pp. Madison, WI.

U.S. FOREST PRODUCTS LABORATORY. 1974. Wood handbook: Wood as an engineering material. USDA Agr. Handbook No. 72, rev. U.S. For. Prod. Lab., Madison, WI.